IOPscience iopscience.iop.org

Home Search Collections Journals About Contact us My IOPscience

On the propagator of Sierpinski gaskets

This article has been downloaded from IOPscience. Please scroll down to see the full text article.

1991 J. Phys. A: Math. Gen. 24 4835

(http://iopscience.iop.org/0305-4470/24/20/016)

View the table of contents for this issue, or go to the journal homepage for more

Download details:
IP Address: 129.252.86.83
The article was downloaded on 01/06/2010 at 13:57

Please note that terms and conditions apply.

J. Phys. A: Math. Gen. 24 (1991) 4835-4842. Printed in the UK

On the propagator of Sierpinski gaskets

J Klafter†, G Zumofen‡ and A Blumen§

† School of Chemistry, Tel-Aviv University, Tel-Aviv, 69978 Israel
‡ Laboratorium für Physikalische Chemie, ETH-Zentrum, CH-8092 Zürich, Switzerland
§ Physics Institute and BIMF, University of Bayreuth, W-8580 Bayreuth, Federal Republic of Germany

Received 21 May 1991

Abstract. In this paper we present numerical calculations for the propagator $P(r, t)$, the probability to reach a distance r at time t having started at the origin at $t = 0$, on Sierpinski gaskets. The results are confronted with approximate analytical expressions. It is shown that $P(r, t) \sim t^{-d_s/2}\Pi(\xi)$, where ξ is the scaling variable: $\xi = r/t^{1/d_w}$. In the short-ξ regime the scaling function follows the form $\Pi(\xi) \sim \exp(-c_1\xi^{d_w})$, while for large ξ, $\Pi(\xi)$ is given asymptotically by $\Pi(\xi) \sim \xi^{\alpha}\exp(-c_2\xi^{\nu})$, with $\alpha = (d_f - d_w/2)/(d_w - 1)$ and $\nu = d_w/(d_w - 1)$. This result extends the previously derived expressions. The numerically observed oscillations which are superimposed on the power-law decay of the autocorrelation function $P(r = 0, t)$ are analysed in terms of typical residence times on hierarchical substructures.

Fractals have been extensively studied as models for geometrically disordered systems. They are known to display anomalous diffusion which is characterized by the sublinear, dispersive behaviour of the time evolution of the mean-squared displacement [1]

$$\langle r^2(t)\rangle \sim t^{2/d_w} \tag{1}$$

with $d_w > 2$. Here, $d_w = 2d_f/d_s$, where d_f is the fractal dimension and d_s the spectral dimension. Equation (1) follows from the scaling properties of the fractal structure, whose d_w value can in general be determined by renormalization techniques [1].

Another quantity of interest is the (ensemble averaged) autocorrelation function $P(0, t)$, the probability to be at the origin at time t having started at the origin at $t = 0$. $P(0, t)$ is related to the vibrational density of states of the fractal and to the mean number of sites visited by a random walker of the structure. $P(0, t)$ has been shown to scale according to [1, 2]

$$P(0, t) \sim t^{-d_s/2}. \tag{2}$$

A more complicated and still open question is the nature of the propagator $P(r, t)$, the (ensemble averaged) probability to reach a distance r at time t having started at the origin at time zero. Several derivations have been proposed for $P(r, t)$, which lead to the relation [1]

$$P(r, t) \sim t^{-d_s/2}\Pi(\xi) \tag{3}$$

where the scaling variable ξ of the scaling function Π is $\xi = r/t^{1/d_w}$. This choice is dictated by the fact that the prefactor of Π in (3) has to agree with (2) and the second moment has to be compatible with (1).

0305-4470/91/204835+08$03.50 © 1991 IOP Publishing Ltd

A stretched exponential form is generally accepted for the scaling function, i.e. $\Pi(\xi) \sim \exp(-C\xi^{\nu})$. Banavar and Willemsen [3] (BW) based their analysis on the Chapman-Kolmogorov relation (CKR) and found the exponent ν to be $\nu = d_w$. O'Shaugnessy and Procaccia [4, 5] (OP) introduced the generalized diffusion equation

$$\frac{\partial P_{OP}(r, t)}{\partial t} = r^{1-d_f} \frac{\partial}{\partial r} K r^{1+d_f-d_w} \frac{\partial P_{OP}(r, t)}{\partial r} \tag{4}$$

where K is a generalized diffusion coefficient. The solution of this partial differential equation is straightforward, leading to

$$P_{OP}(r, t) \sim t^{-d_s/2} \exp(-C_{OP}\xi^{d_w}) \tag{5}$$

which obeys the form proposed by Banavar and Willemsen [3]. Furthermore, in [5] the constant C_{OP} was calculated for a particular symmetric location of the origin (as is given in figure 1(a)), which resulted in

$$C_{OP} = (d+1)d_f(d_w - d_f)\tau/d_w^2. \tag{6}$$

A different form for $P(r, t)$ was obtained by Guyer [6], who started from numerical renormalization results in the Laplace space. He proposed the form

$$P_G(r, u) \sim u^{d_s/2-1} \exp(-C_G r u^{\beta}) \tag{7}$$

where u is the Laplace variable, $P_G(r, u)$ is the Laplace transform of $P_G(r, t)$ and $\beta = 1/d_w$. Guyer calculated $P(r, t)$ in the time domain by first inverting the power law and the exponential separately and then inferred that approximately

$$P_G(r, t) \sim t^{-d_s/2} \exp(-a_1\xi^{\nu}) \tag{8}$$

where now the exponent ν equals $d_w/(d_w - 1)$. Recently, Van den Broeck [7, 8] also obtained the form given in (7) by analytical renormalization considerations. Furthermore, (8) was also derived by Barlow and Perkins (BP) [9]. Evidently, there is a discrepancy between the ν-values reported by BW and OP on the one hand and by Guyer, Van den Broeck and BP on the other; this leads to the observation that these forms are limiting laws and to the fit of the numerical results by a single averaged exponent $\bar{\nu}$ intermediate between the two forms [1, 10].

Recently, the propagator $P(r, t)$ has attracted much attention in the analysis of both the transient [11, 12] and the steady state [13] $A + B \to 0$ reaction; in the former $P(r, t)$ plays a major role in the calculation of the density-difference function [11, 12], whereas for the latter the generalized diffusion operator of (4) was used [13]. Furthermore, $P(r, t)$ appears in studies of superlocalization in the hopping conductivity on fractal media [10, 14].

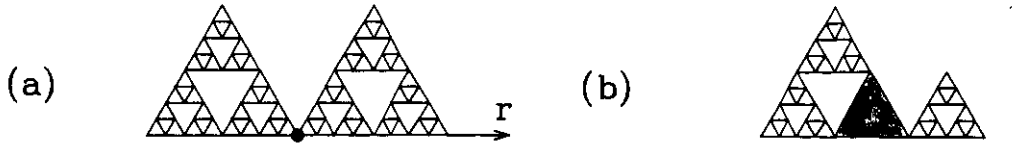

Figure 1. Schematic representation of the Sierpinski gasket structures used in the numerical calculation. (a) The origin chosen in the numerical calculation of $P(r, t)$ is denoted by a dot and the r-axis is as indicated. (b) The structure used to calculate $P(0, t)$ with origins chosen within the shaded area in order to avoid finite size effects.

The purpose of this paper is to find $P(r, t)$ numerically on Sierpinski gaskets and to compare the results with approximate analytical forms. In particular we highlight the cross-over in the behaviour of $P(r, t)$ between the small- and the large-ξ regimes and analyse it in detail.

We now study numerically the propagator $P(\boldsymbol{r}, t; \boldsymbol{r}_0, t_0)$ for continuous time random walks (CTRWs) on Sierpinski gaskets by solving the master equation

$$\dot{P}(\boldsymbol{r}, t; \boldsymbol{r}_0, t_0) = (2d\tau)^{-1} \sum_{\boldsymbol{r}_1} [P(\boldsymbol{r}_1, t; \boldsymbol{r}_0, t_0) - P(\boldsymbol{r}, t; \boldsymbol{r}_0, t_0)] \tag{9}$$

where the sum runs over the nearest neighbours of site $\boldsymbol{r}$, d is the Euclidean dimension and τ the hopping time. As initial condition we take

$$P(\boldsymbol{r}, 0; \boldsymbol{r}_0, 0) = \delta_{\boldsymbol{r},\boldsymbol{r}_0}. \tag{10}$$

In general, one should note that $P(r, t)$ as used above is the radial average of $P(\boldsymbol{r}, t)$, which itself is a structure-averaged quantity, $\langle P(\boldsymbol{r}+\boldsymbol{r}_0, t; \boldsymbol{r}_0, 0)\rangle_{\boldsymbol{r}_0}$. Similarly, $P(0, t)$ in (2) is also a structure-averaged function: $\langle P(\boldsymbol{r}, t; \boldsymbol{r}, t)\rangle_{\boldsymbol{r}}$. In our numerical calculation we choose for $\boldsymbol{r}_0$ in (9) a symmetric point, which is at the top of one of the main triangles and for the presentation of the r-dependence of $P(\boldsymbol{r}, t; \boldsymbol{r}_0, 0)$ an axis along the side of the main triangle, as indicated in figure 1(a). For this particular condition we denote the numerical propagator by $P(r, t)$. In the numerical realization use was made of the symmetry of the problem so that only one main triangle was considered in the computation of $P(r, t)$.

Proceeding, we will compare the numerical results with the analytical forms given in (5), (7) and (8). Moreover, as discussed in the appendix, we also consider the expression

$$P_{\mathrm{sp}}(r, t) \sim a_0 t^{-d_s/2} \xi^{\alpha} \exp(-a_1 \xi^{\nu}) \tag{11}$$

where ν is still $\nu = d_{\mathrm{w}}/(d_{\mathrm{w}}-1)$ and α is given by $\alpha = (d_{\mathrm{f}} - d_{\mathrm{w}}/2)/(d_{\mathrm{w}}-1)$. Equation (11) differs from the scaling form (8) by the term ξ^{α} in front of the exponent. Our study in the appendix suggests that (11) is exact to first order, and from the comparison to the simulation calculations the prefactor ξ^{α} turns out to be significant. (Higher-order terms to (11) can be calculated in principle but they do not improve the description significantly, since Guyer's form, (7), is itself an approximation.) In order to establish the range of validity of the small- and large-ξ regimes and to highlight the cross-over behaviour of $P(r, t)$ we present our numerical results in three different ways.

In figure 2 we plot for Sierpinski gaskets embedded in $d = 3$ the form $P(r, t)/P(0, t)$ against ξ on linear scales for $t/\tau = 10$, 10^2, 10^3 and 10^4. The numerical results are compared with the approximate forms $P_{\mathrm{OP}}(r, t)$, $P_{\mathrm{G}}(r, t)$, (obtained from direct Laplace inversion of (7)), and $P_{\mathrm{sp}}(r, t)$. The plotted curves demonstrate that for small ξ-values the OP-approximation describes the simulation results quite well. Systematic deviations are obvious for large ξ. It appears that generally the scaling behaviour of $P(r, t)$ with ξ is more pronounced for large ξ-values. Furthermore, in the range where $P_{\mathrm{G}}(r, t)$ represents $P(r, t)$ well, $P_{\mathrm{sp}}(r, t)$ approximates it well too. At $r = 0$ the slopes of $P_{\mathrm{G}}(r, t)$ and of $P_{\mathrm{sp}}(r, t)$ deviate from zero but one should bear in mind that these forms are valid for the large-r regime. Obviously, such moments which are dominated by the central part of $P(r, t)$ can be determined satisfactorily from $P_{\mathrm{OP}}(r, t)$ while the moments, which are determined mainly by the wings of the distribution, cannot be obtained from $P_{\mathrm{OP}}(r, t)$ alone [6].

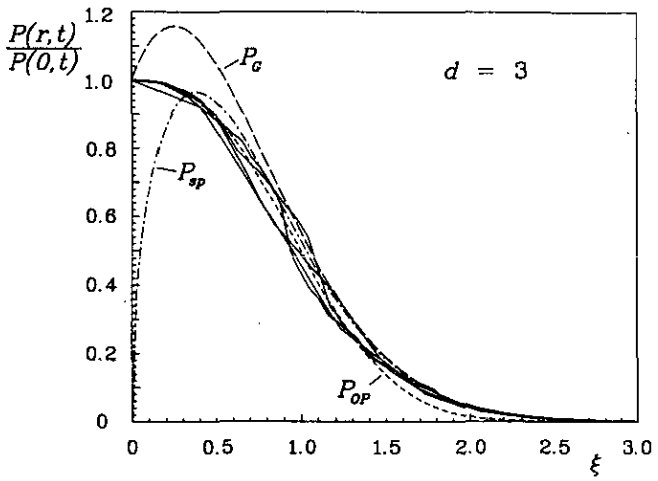

Figure 2. The propagator $P(r, t)$ on linear scales. Plotted are $P(r, t)/P(0, t)$ against the scaling variable ξ for times $t/\tau = 10, 10^2, 10^3, 10^4$ and for the embedding dimension $d = 3$. The short-broken line gives $P_{OP}(r, t)$, the chain line indicates the $P_G(r, t)$, and the long-broken line denotes $P_{sp}(r, t)$.

In order to show the variation of the exponent ν, we plotted in figure 3 on log–log scales $P(r, t)/P(0, t)$ against ξ. As in figure 2, the simulation results are confronted with approximate forms. We notice that each of the two forms, P_{OP} and P_G, fits the simulation results in a different regime. To show the slow convergence of ν the effective exponent, $\nu_{eff} = \partial \ln\{-\ln[P_G(r, t)/P_G(0, t)]\}/\partial \ln t$, is plotted in the insert. The two broken lines given in the insert indicate the lower and the upper bounds, $d_w/(d_w - 1)$ and d_w, respectively.

To illustrate more clearly the validity ranges of the two approximate forms $P_{OP}(r, t)$ and $P_G(r, t)$ we plotted in figure 4 $-\ln[P(r, t)/P(0, t)]C_{OP}\xi^{d_w}$ as full lines and $\ln[P(r, t)/P(0, t)]/\ln[P_G(r, t)/P_G(0, t)]$ as broken lines. If the theoretical predictions hold exactly, horizontal lines at an ordinate value of unity would appear. The full

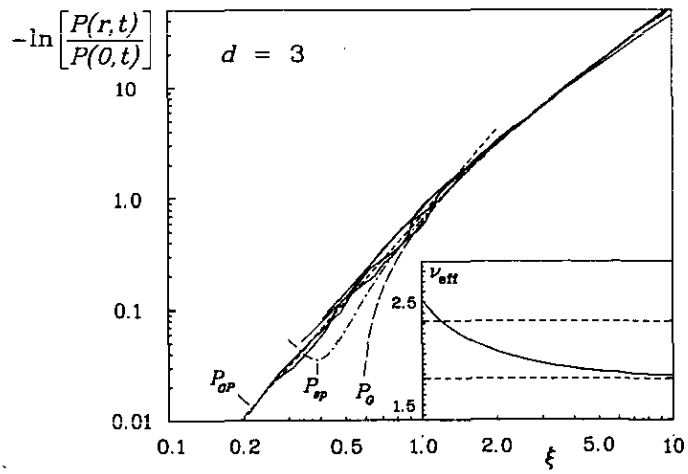

Figure 3. As in figure 2 but on log–log scales. The insert shows the effective exponent ν_{eff} and the broken lines in the insert denote the lower bound $\nu = d_w/(d_w - 1)$, and the upper bound $\nu = d_w$, respectively.

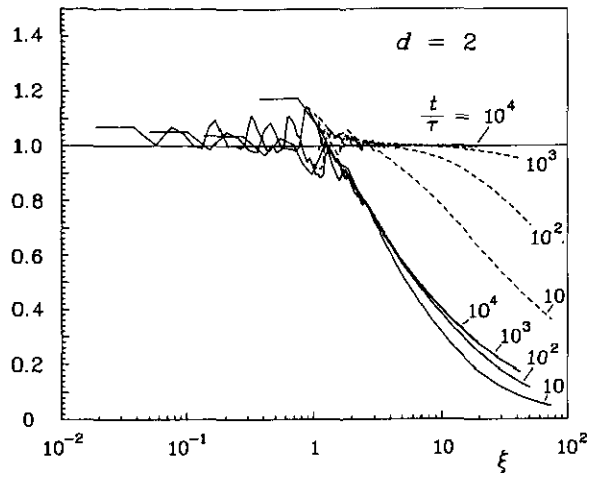

Figure 4. The cross-over behaviour between different ξ-regimes. Plotted are the ratios of the simulation results over the expected theoretical predictions $\ln[P(r, t)/P(0, t)]/\ln[P_x(r, t)/P_x(0, t)]$: full lines for $x = \text{OP}$ and broken lines for $x = \text{G}$. The times chosen are as indicated.

lines show a marked cross-over behaviour at $\xi \simeq 1$, clearly indicating that $P_{\text{OP}}(r, t)$ holds only for $\xi < 1$. The broken lines illustrate that $P_{\text{G}}(r, t)$ applies for $\xi > 1$ and that the asymptotic description holds better at longer times. This is due to the fact that the asymptotic form is valid for $r < t/\tau$ if compared with discrete lattice results from CTRW. We point out that for fixed stepping frequencies one has $P(r, t) = 0$ for $r > t/\tau$. Here the largest value of r is $r_{\max} = 1028$ while the values of t were: $t/\tau = 10$, 10^2, 10^3 and 10^4. Only for $t/\tau = 10^4$ is $r_{\max} < t/\tau$ obeyed. The figure shows that the constant C_{OP} fits the result to an accuracy of 5%. For $d = 3$ the fit is better while for $d = 4$ it is off by 20%. Numerically determined values of C_{G} are given in table 1; in this case of $d = 2$ the C_{G} value agrees with that given by Van den Broeck [8].

We now turn to the question whether the CKR provides any information about $P(r, t)$. The CKR was considered by Banavar and Willemsen [3] to obtain the exponent $\nu = d_w$ and was also discussed by Guyer [6]. For discrete lattices, the CKR takes the form

$$P(\boldsymbol{r}, t; \boldsymbol{r}_0, 0) = \sum_{\boldsymbol{r}_1} P(\boldsymbol{r}, t; \boldsymbol{r}_1, t_1) P(\boldsymbol{r}_1, t_1; \boldsymbol{r}_0, 0) \qquad t \geq t_1 \geq 0 \tag{12}$$

where $\boldsymbol{r}_1$ runs over all lattice sites. For the particular case $\boldsymbol{r} = \boldsymbol{r}_0$ and $t = 2t_1$, and considering the symmetry of the propagator, $P(\boldsymbol{r}, t; \boldsymbol{r}_0, 0) = P(\boldsymbol{r}_0, t; \boldsymbol{r}, 0)$ from (9), one has

$$P(\boldsymbol{r}, 2t; \boldsymbol{r}, 0) = \sum_{\boldsymbol{r}_1} P^2(\boldsymbol{r}, t; \boldsymbol{r}_1, 0) \tag{13}$$

Table 1. Exponential prefactors which enter in (6) and (7).

d	C_{OP}	C_{G}
2	0.650	1.96[a]
3	0.700	2.30
4	0.715	2.56

[a] In agreement with the value reported in [8].

and the structural average of the RHS of (13) gives

$$\left\langle \sum_{r_1} P^2(r, t; r_1, 0) \right\rangle_r = \langle P(r, 2t; r, 0) \rangle_r = P(0, 2t). \tag{14}$$

This relationship appears in the derivation of the density-difference function in the transient $A+B \rightarrow 0$ reaction [11, 12]. Thus, a detailed analysis of $P(0, t)$ is important. Interestingly, for Sierpinski gaskets $P(0, t)$ does not follow a simple form but rather shows oscillations superimposed on the power-law decay as previously observed [5]. The periods of the oscillations are related to the typical time spent on a hierarchical substructure. In order to study the periods we propose the following hierarchical approach. We denote by τ_n the characteristic time the particle needs to traverse the substructure at the nth iteration. Thus

$$\tau_{n+1}/\tau_n = 2^{d_w} = d+3 \tag{15}$$

where use was made of the fact that for Sierpinski gaskets $d_w = \ln(d+3)/\ln(2)$. We further assume that all sites of a substructure at the nth iteration are equally populated for times t: $\tau_n < t < \tau_{n+1}$ and take for the number of sites of a substructure the asymptotic value $(d+1)^n$. An approximate form for the autocorrelation function can thus be written as a sum of exponentials:

$$P(0, t) = b \sum_n (d+1)^{-n} \exp[-(d+3)^{-n} \phi t/\tau] \tag{16}$$

where b is a constant and ϕ acts as a phaseshift on a logarithmic time-scale. To reconcile the power-law decay we replace the sum by an integration and find

$$P(0, t) \sim B(t/\tau)^{-d_s/2} \tag{17}$$

with

$$B = b\Gamma(d_s/2)/[\phi^{d_s/2} \ln(d+3)]$$

where $d_s = 2\ln(d+1)/\ln(d+3)$ is the spectral dimension of the Sierpinski gasket. In table 2 the constants b, ϕ and B are collected for several embedding dimensions d. The constants b and ϕ were adjusted to results obtained from the numerical solution of (9) for origins chosen randomly (to avoid finite size effects) in the centre substructure as demonstrated in figure 1(b) and averages were taken over 100 different origins.

Figure 5 shows the numerical results and an analysis of the oscillations. Plotted are $P(0, t)t^{d_s/2}$ against t on linear scales for several embedding dimensions d. The oscillations are clearly visible in the figure and it turns out that the structural average does not wash out the oscillatory behaviour. The approximate form given by sums of exponentials, (16), and indicated by broken lines, reproduces the periods for all d. For small dimensions d there are deviations between the calculated and the

Table 2. Constants which enter in (16) and (17).

d	b	ϕ	B
2	0.439	1.30	0.302
3	0.355	0.95	0.246
4	0.323	0.89	0.207
6	0.246	0.75	0.156
13	0.134	0.62	0.078

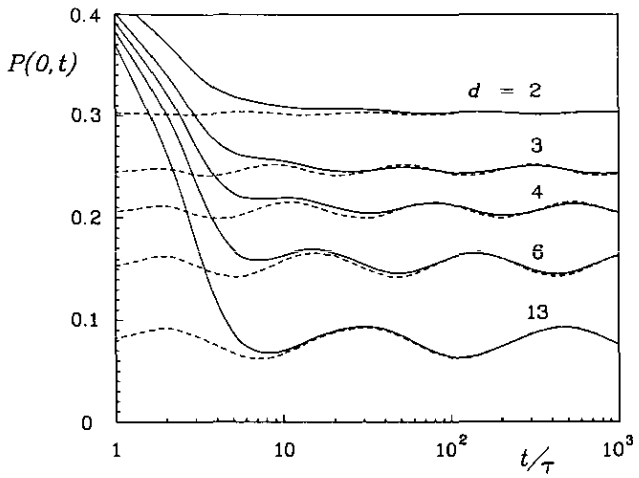

Figure 5. Structure-averaged autocorrelation function plotted as $P(0, t)t^{d_s/2}$. Full lines for $P(0, t)$ taken from simulation calculations and broken lines for $P(0, t)$ calculated from (16). The dimensions d are as indicated.

simulated $P(0, t)$ amplitudes but the agreement becomes much better with increasing dimension d.

In summary, the propagator $P(r, t)$ shows clearly two different regimes. As long as $\xi \ll 1$, $P(r, t)$ obeys the Banavar-Willemsen and O'Shaugnessy–Procaccia form quite well; for $\xi \gg 1$ the behaviour of $P(r, t)$ is described by the Guyer form. The diffusion equation put forward by O'Shaugnessy and Procaccia is appropriate in treating the diffusion on small length scales; however, it is not valid for large r distances. This explains why $P_{OP}(r, t)$ is a good approximate form for small ξ. In the large-ξ regime the correct first-order term obtained from the saddle point approximation to the Guyer form, (11), provides a reasonable description of the decay. In fact it turns out that the additional power is important in the description and thus this problem is comparable to the problems encountered in two different fields: in the trapping problem in 1D [15] and in the description of the propagator for enhanced diffusion in random velocity fields [16]. Furthermore, the autocorrelation function $P(0, t)$ can be described by a sum of exponentials, which is useful in higher dimensions d, where the numerical calculations are not easily extended to long times.

Acknowledgments

A grant of computer time from the Rechenzentrum der ETH-Zürich and the support of the Deutsche Forschungsgemeinschaft (SFB 213) and of the Fonds der Chemischen Industrie are gratefully acknowledged. JK acknowledges the support of the Fund for Basic Research administered by the Israel Academy of Sciences and Humanities.

Appendix

In this appendix we derive the first-order correction term of the large-ξ behaviour of $P(r, t)$. We use the saddle-point approximation for the Laplace inversion of the form proposed by Guyer [6] given in (7) of the main text:

$$P(r, u) = Au^{d_s/2-1} \exp(-C_G r u^{\beta}) \qquad r \geq 0 \tag{A1}$$

where A is a normalization constant. We follow the methods discussed by Daniels [17] and Helfland [18] and write the Laplace inverted form as the integral:

$$P(r, t) = A/(2\pi i) \int_{c-i\infty}^{c+i\infty} du\, u^{d_s/2-1} \exp(-C_G r u^{\beta} + ut). \tag{A2}$$

We introduce two additional functions to write a short form of the integrand:

$$\phi(u)\, e^{-\psi(u)} = u^{d_s/2-1} \exp(-C_G r u^{\beta} + ut) \tag{A3}$$

with $\phi(u) = u^{d_s/2-1}$ and $\psi(u) = C_G r u^{\beta} - ut$. The dominant term of the asymptotic behaviour obtains from the saddle-point approximation which reads

$$P(r, t) \sim \phi(u_0)[2\pi\psi''(u_0)]^{-1/2}\, e^{-\psi(u_0)}. \tag{A4}$$

Although the integration has to be taken along a path in the complex plane, the case considered here is simple because the saddle point is on the real axis, as follows from symmetry arguments. Thus, the saddle point is obtained by setting the first derivative to zero:

$$\psi'(u)\big|_{u=u_0} = \beta C_G r u^{\beta-1} - t\big|_{u=u_0} = 0. \tag{A5}$$

Solving for u_0 and inserting u_0 into (A4) gives

$$P(r, t) \sim a_0 t^{-d_s/2} \xi^{\alpha}\, e^{-a_1 \xi^{\nu}} \tag{A6}$$

with

$$\alpha = (d_f - d_w/2)/(d_w - 1) \qquad \text{and} \qquad \nu = (1-\beta)^{-1} \tag{A7}$$

and with the constants

$$a_0 = A[2\pi(1-\beta)]^{-1/2}(\beta C_G)^{\alpha} \qquad a_1 = (d_w - 1)(\beta C_G)^{\nu}. \tag{A8}$$

These constants were used to calculate $P_{sp}(r, t)$ in figures 2 and 3 and to fit the coefficients C_G, which are presented in table 1 for $d = 3$ and 4.

References

[1] Havlin S and Ben-Avraham D 1987 *Adv. Phys.* **36** 695
[2] Alexander S and Orbach R 1982 *J. Phys. Lett., Paris* **43** L625
[3] Banavar J R and Willemsen J F 1984 *Phys. Rev.* B **30** 6778
[4] O'Shaugnessy B and Procaccia I 1985 *Phys. Rev. Lett.* **54** 455
[5] O'Shaugnessy B and Procaccia I 1985 *Phys. Rev.* A **32** 3073
[6] Guyer R A 1985 *Phys. Rev.* A **32** 2324
[7] Van den Broeck C 1989 *Phys. Rev. Lett.* **62** 1421
[8] Van den Broeck C 1989 *Phys. Rev.* A **40** 7334
[9] Barlow M T and Perkins E A 1988 *Probab. Th. Rel. Fields* **79** 543
[10] Brooks Harris A and Aharony A 1987 *Europhys. Lett.* **4** 1355
[11] Sokolov I M and Blumen A 1991 *Phys. Rev.* A **43** 2714
[12] Zumofen G, Klafter J and Blumen A *J. Stat. Phys.* in press
[13] Clément E, Sander L M and Kopelman R 1989 *Phys. Rev.* A **39** 6472
[14] Deutscher G, Lévy Y and Souillard B 1987 *Europhys. Lett.* **4** 577
[15] Anlauf J K 1984 *Phys. Rev. Lett.* **52** 1845
[16] Zumofen G, Klafter J and Blumen A 1990 *Phys. Rev.* A **42** 4601
[17] Daniels H E 1954 *Ann. Math. Stat.* **25** 631
[18] Helfland E 1983 *J. Chem. Phys.* **78** 1931